Numerical simulation of the effect of column removal on the plastic rotation of beams in reinforced concrete structures

KAHIL. Amar*, MEZIANI. Faroudja

Civil engineering department, faculty of construction engineering, university, Mouloud MAMMERI, Tizi-Ouzou, 15000, Algeria.

Abstract:

In recent years, the progressive component collapse phenomenon in structures have attracted the attention of agencies around the world, structural systems are subject to progressive collapse when they are exposed to excessive loads that exceed the ultimate capacity of the structural elements. The rapid loss of structural components, such as columns, causes failure mechanisms that can result in the total or partial collapse of the structure. Currently, researchers are adopting different modeling techniques to simulate the effect of structural load-bearing elements loss on the overall behavior of structures during a progressive collapse. The objective of this study is to interpret the effect of the deleted column in the reinforced concrete frame structures on the overall behavior. The modeling procedure was implemented following the finite element method. An experimental model was tested to validate the accuracy of the modeling approach using CAST3M, in which the local modeling approach (fiber model) for the cross-sections and the global modeling approach for the elements (beams and columns) were used. The behavior laws are used with the aim of modeling the behavior of the materials using empirical laws during their deformations. Then, the study focused on the study of the plastic hinges development under vertical loading (imposed displacement) in a reinforced concrete frame composed of three stories and four spans. The results show that the occurrence of plastic hinges (damage level) is located on the near-central column nodes. At the edges, minor damage is noted, remaining practically in the elastic stage.

Keywords:

Concrete frame, progressive collapse, damage level, multi-fiber approach.

* amar.kahil@yahoo.com

1. Introduction

During their lifetime, large structures are susceptible to undergo accidental loads, such as explosions or impacts. These structures columns can exhibit damage (loss in bearing capacity) after the application of extreme loads, which can result in a significant increase in the bending moments of the adjacent structural elements [1-3]. For a reinforced concrete frame designed to support dead loads, the beams adjacent to the damaged area (near the removed column) [4, 5] are just slightly capable of resisting the additional bending moment and are likely to propagate the damage until the structure collapses, such a collapse is known as a progressive collapse [6-8].This latter is defined as the propagation of an initial local failure (plastic hinge) from one element to another, leading to the partial or total collapse of a structure[9].

The progressive collapse is a disastrous structural phenomenon that can occur due to human mistakes or natural incidents. A local collapse of an element generates significant deformations that lead eventually to the collapse of the structure [10-12]. This is a rare phenomenon in which the whole or at least a large part of the structure fails due to the collapse of a small part. The progressive collapse, as a result of inappropriate design, and building mistakes can result in tremendous economic losses and casualties.

Mechanical testing and numerical simulation are two main techniques to study the resistance of structures to a progressive collapse [13-16]. For a numerical simulation, a linear static, a nonlinear static, a linear dynamic, and a nonlinear dynamic analysis can be used to study the response of buildings under a progressive collapse [17-20].

Static analysis procedures such as the pushover analysis [21-24] are independent of a load history. In addition, many of the static analysis procedures [25-27] do not model the impact of failed components after the initial partial collapse. While a nonlinear dynamic analysis [28-30] can precisely predict the progressive collapse, it is complex to conduct and involves high computational costs.

This paper presents a non-linear static model for the analysis of the collapse of reinforced concrete frames undergoing a column failure (removal). It is based on a damage assessment that takes into account the combined effects of bending forces in accordance with FEMA 273[31].

The modeling was carried out using a finite element procedure, and the experimental model tests to validate the precision of the modeling approach, with the calculation code CAST3M, in which, the fiber model has been used [32, 33]. Then, an RC frame with 3 spans and 3 stories was modeled following the same procedure, in order to display the impact of the first-story central-column removal on the damage and development of the plastic hinges in the adjacent beams of the different stories.

For reinforced concrete framed structures, if the live loads applied to a sound structure are significant, they can have significant effects on the damage of the structure after the column is removed. To take into account this type of loading, an imposed displacement at the top of the RC structure above the central column is applied, and the damage caused by the appearance of plastic hinges in the beams is illustrated.

2. Calculation of the plastic rotation

The strain energy in the structure is dissipated by the formation of plastic hinges in the end zones of an element without affecting the rest of the structure. Several analytical models [34-39] have developed semi-empirical formulae (analytical models) to estimate the plastic rotation θ_p [40, 41].

The rotation of an element can be determined from the curvature distribution along the length of the element [42, 43]. Therefore, the rotation between two points, A and B (Figure 1) is equal to the area under the curve between these two points, analytically it is given by equation 1.

$$\theta_{AB} = \int_{A}^{B} \phi(x)\, dx \qquad (1)$$

Where θ is the rotation of an element, x distance of the elementary element dx from B, and ϕ is the curvature between points A and B (see figure 1.c).

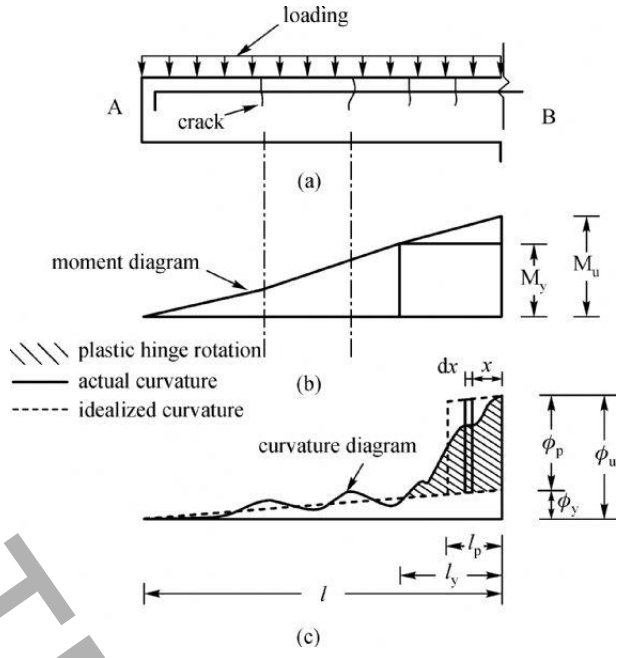

Fig. 1. Curvature and bending moment distribution along the length of an element

There is a large increase in curvature observed at the moment of perpetration in the plastic range (in the vicinity of the yield stress) of the tense steel. At the vicinity of the ultimate load, the value of the curvature increases suddenly, causing large plastic deformations. Since the concrete around the cracks can carry some tension (tension-stiffening), a fluctuation of the curvature along the component length can be noted. Each of the curvature peaks corresponds to a crack. The actual curvature distribution at the ultimate load region is simplified into elastic and plastic regions (Figure 1.c), thus the total rotation (θ_t) over the component length can be divided into elastic and plastic rotations. The elastic rotation (θ_e), (before reaching the yield stress of the reinforcements) can be obtained using the curvature at yield. The plastic rotation can be determined, on each side of a section, by equation 2, [34, 42].

$$\theta_p = \int_0^{ly} \left| \phi(x) - \phi_y \right| dx \tag{2}$$

Where $\phi(x)$ is the curvature at distance x from the section at the ultimate load, ϕ_y is the curvature at yield, and ly is the length of the component segment over which the maximum moment exceeds the yield moment (yielding length). The hatched area in figure 1.c is the plastic rotation (θ_p), which occurs after the elastic rotation of the plastic hinge at the ultimate load [34, 42].

3. Plastic hinge capacities provisions for RC components by FEMA 273

The FEMA nonlinear procedures require the definition of a load-deformation relation. Such a curve is given in figure 2.

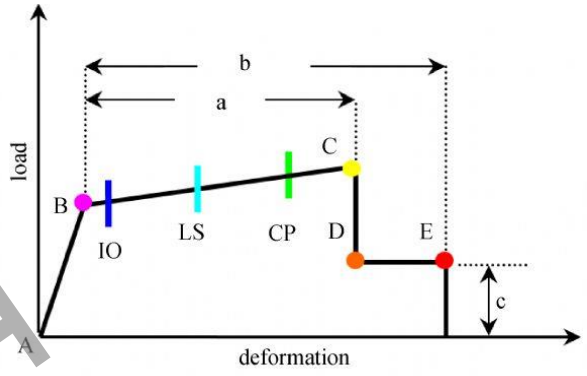

Fig. 2. Typical load-deformation relation and target performance levels

Point A corresponds to the unloaded condition. Point B corresponds to the nominal steel yield strength. The slope of segment BC is usually taken between 0% and 10% of the initial slope (segment AB). Point C has a resistance equal to the ultimate strength. Segment CD corresponds to the initial failure of the component. It can be associated with flexural reinforcement failure, concrete debonding or shear failure. Segment DE represents the residual strength of the member and point E corresponds to the deformation limit [31]. However, we usually consider the initial failure as well as the deformation limit at point C, and therefore points E, D and C have the same deformation.

Four levels of performance, O, IO, LS, and CP were considered as specified in the FEMA-356, ATC-40, and FEMA-440 international codes (see table 1).

Table 1. Performance levels according to FEMA 440

Level	Definition
Occupancy (O)	Absence of damage.
Immediate Occupancy (IO)	Has very slight damage with minor local deformations and negligible residual drift.
Life Safety (LS)	Defines the limit beyond yield stress that the section is capable of safely sustaining.
Collapse Prevention (CP)	Collapse prevention is associated with extensive inelastic deformations of structural elements.

As the damage level 'O' corresponds to the absence of damage, in this study, the failure related to the items: Immediate Occupancy (IO), Life Safety (LS), and Collapse Prevention (CP), was used to define the plastic hinge damage level [33]. The plastic-rotation limiting values associated with the damage levels, as prescribed by FEMA 273, are presented in Table 2 [44].

Table 2. FEMA 273 acceptance criteria for reinforced concrete beams

Damage level	Plastic rotations θp (rad)
Immediate Occupancy	[0.0 , 0.005]
Life Safety	[0.005 , 0.01]
Collapse Prevention	[0.01 , 0.02]

4. Experimental model

The experimental model (figure 3) was based on the program presented by Waleed Mohamed Elsayed [45]. The test specimen consists of a half-scale model of a one-story RC frame structure stretching on two adjacent beam spans resulting from the removal of the central supporting column on the first floor of a building.

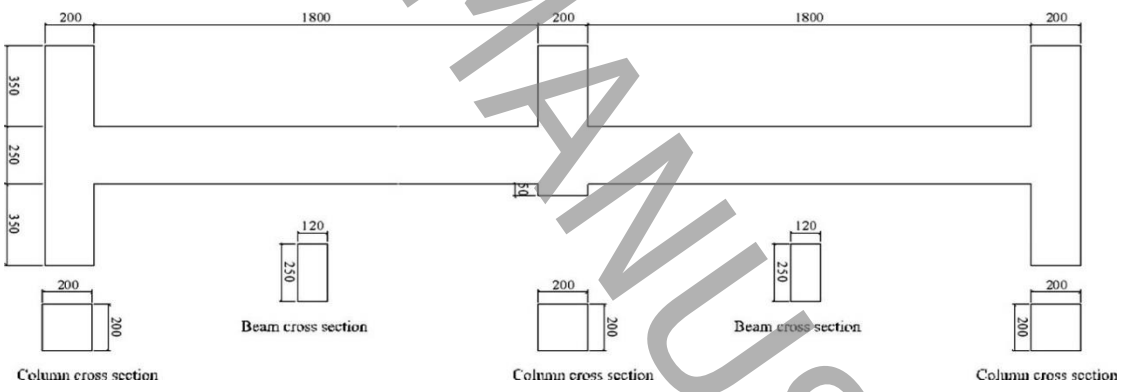

Fig. 3. Test specimen concrete dimensions (mm).

The properties of the reinforcement (Figure 4) of the elements are detailed in tables 3 and 4. A vertical displacement was imposed, and the corresponding load is measured up till the failure of the structure [45].

Table 3. Test specimen properties.

Damage level	Plastic rotations θp (rad)
Immediate Occupancy	[0.0 , 0.005]
Life Safety	[0.005 , 0.01]
Collapse Prevention	[0.01 , 0.02]

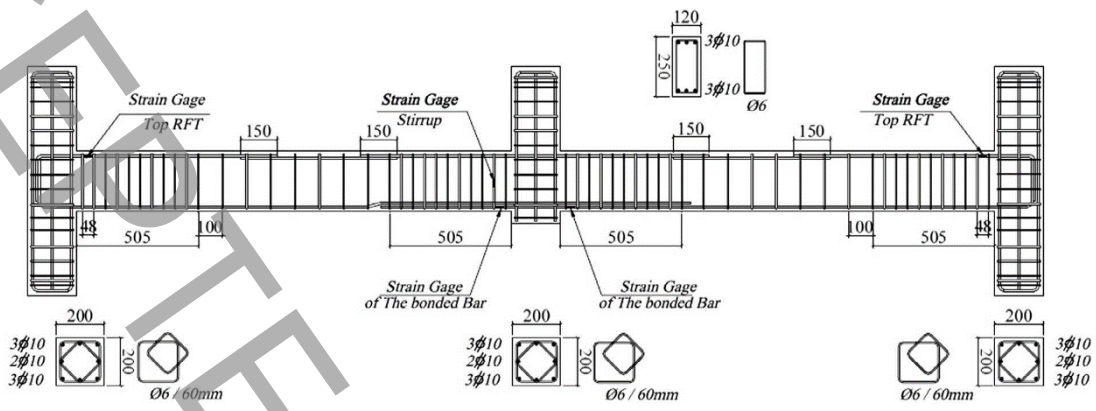

Fig. 4. Reinforcement details of the tested RCF S2.

Table 4. Properties of reinforcement steel.

Test specimen	F_{cu} (MPa)	Longitudinal bars and reinforcement ratio		Ties and Φ@mm
S2	43.7	Top bars RFT (%) 3Φ10 (0.78%)	Bottom bars adjacent to middle column RFT (%) 6Φ10 (1.57%)	Φ6@50

5. Multi-fiber approach simulation of the experimental RC frame

5-1- Multi-fiber modeling

To perform a 3D non-linear analysis of the concrete structure behavior, the multi-fiber approach (Figure 6) was adopted [33, 40]. Although the spatial representation is simplified, the inelastic behavior of concrete was correctly represented. The multi-fiber approach allows the non-linear behavior of materials to be taken into an account.

In the present study, the Timoshenko beam element was used, in contrast with the Euler-Bernoulli hypothesis; it takes into account the shear effects. The element cross-section is described using two-dimensional elements (3 or 4 nodes), and each fiber is associated with a non-linear uniaxial law which represents the non-linear concrete and/or steel behavior (figure 5).

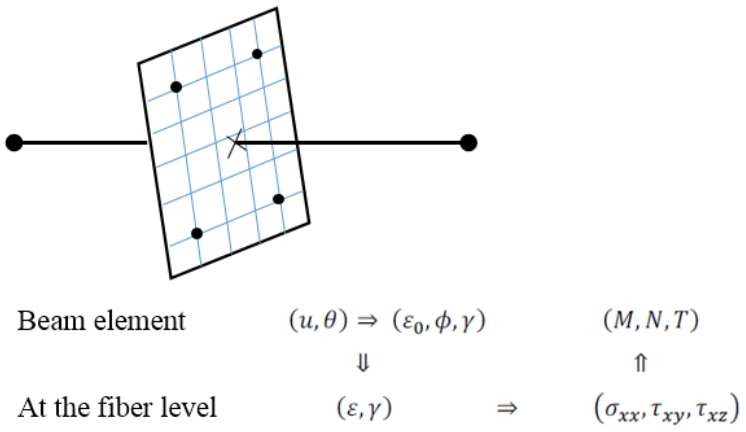

Fig. 5. Description of a multi-fiber beam model

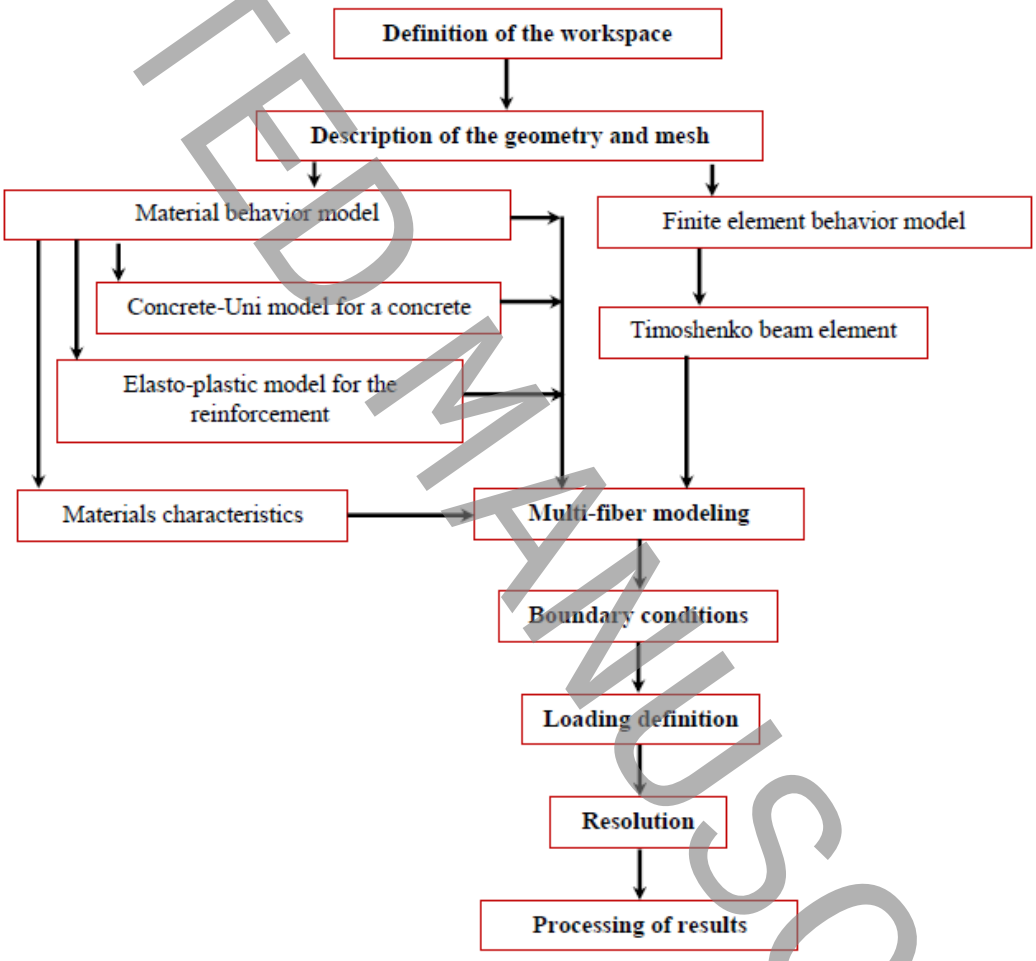

Fig. 6. Flowchart of the finite element code CAST3M.

5-2- Behavior laws

The models that exist in CAST3M code library are adopted in this study, namely Concrete-Uni for the concrete and an elastoplastic model for the reinforcement.

The Concrete-Uni Model (Figure 7) relies on the model of Hognestad [46] which is capable of representing the behavior of the confined and unconfined concrete in compression [47]. The Concrete-Uni Model also allows to reproduce the softening phenomenon after cracking. Indeed, the unilateral behavior of the concrete (the reclosing of the cracks), as well as the softening after the compressive strength limit, is well reproduced by this model. The modeling of transverse reinforcement (figure 8) is ensured for its part in this model by the notion of confined concrete [48, 49].

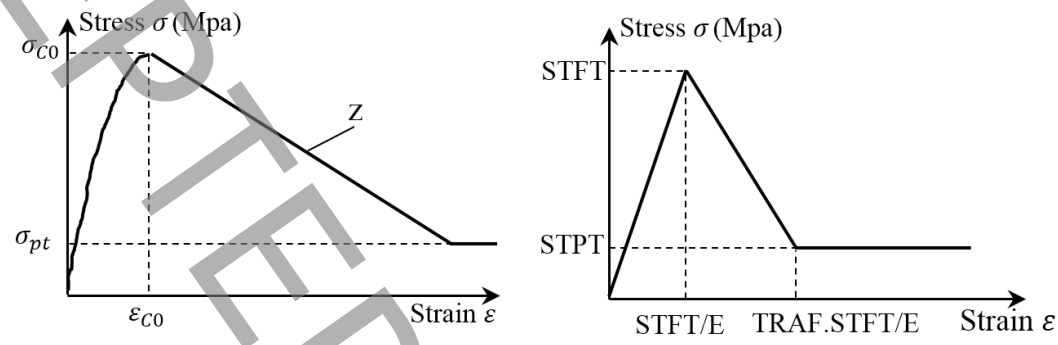

Fig. 7. Behavior laws used for concrete

Concerning the reinforcement, the elastoplastic model (Figure 8) with kinematic hardening (Steel-Perfect), available in the software, was selected for the modeling [48, 49].

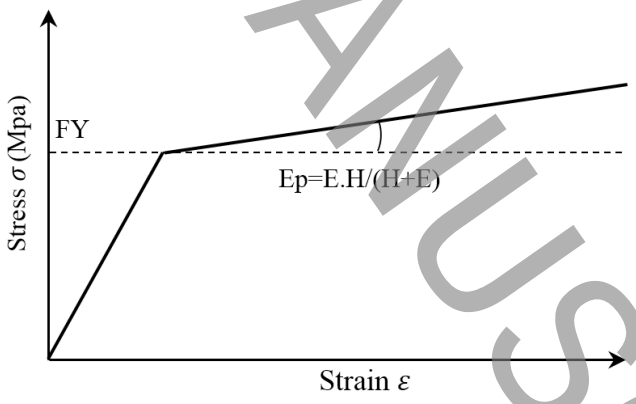

Fig. 8. Behavior law used for the reinforcement

5-3- Loading and boundary conditions

The two short outer columns were blocked against any horizontal and vertical displacement during the analysis, and an imposed displacement was applied to the middle column section to simulate the effect of vertical loads (figure 9).

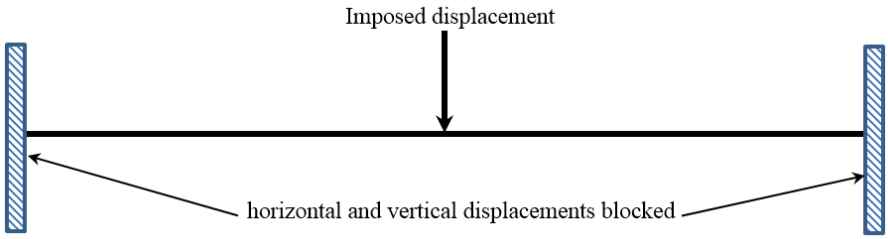

Fig. 9. Static diagram of boundary conditions and loading

5-4- Experimental RC frame test results

Figure 10 represents the comparison between the numerical and the experimental results. Globally, the numerical model can predict, acceptably, the elastic and the plastic response of the experimental RC frame. The numerical model accurately predicts the failure load of the beams, as shown in figure 10. The values of failure loads recorded for both the experimental and simulation are summarized in table 5.

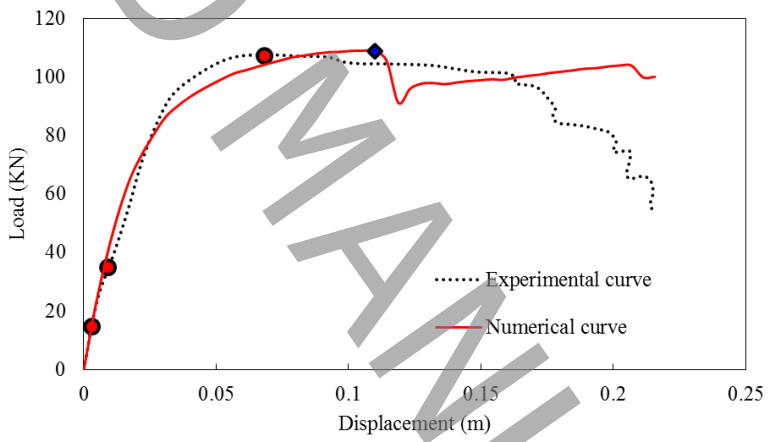

Fig. 10. Comparison between numerical and experimental in terms of failure criteria for the beams

Table 5. Values of failure loads for the experimental and numerical simulation.

Points	Experimental observation	Experimental test load (kN)	Numerical simulation load (kN)
1	The first flexure crack developed at the negative moment zone adjacent to the right column [46].	15.00	≈ 15.00
2	The positive moment zone adjacent to the middle column stub showed first crack [46].	35.00	≈ 35.00
3	Crushing of the concrete at the compressive zone adjacent to the middle column stub was observed and the crack at the end of the lap splice of the bottom reinforcement became wider [46].	107.40 Point 3 in figure 10	108.83 Point 4 in figure 10

Table 6 shows the results obtained for the simulated experimental RC frame in terms of damage level according to FEMA 273, the values of the plastic rotations largely exceed the collapse prevention limit values.

Table 6. Plastic rotation and damage level of the tested beams according to FEMA 273.

Beams	Location	Values of θp calculated with finite element model (rad)	Plastic hinges appearance chronology	θp according to FEMA 273 (rad)	Damage level by FEMA 273
1	Left	0.0991	1	> θp (CP)=0.02	Collapse Prevention
	Right	0.0953	2		
2	Left	0.0766	4		
	Right	0.0941	3		

The results in terms of plastic rotation show that the beams of the (beams) first level have larger values of plastic rotations. Indeed, all values are between 0.0766 and 0.0991 rad, these values are always greater than θ_p which corresponds to the prevention of collapse damage level of FEMA 273 [31]. The results dealing with the appearance of plastics hinges (Figure 11) in the vicinity of the nodes are in good agreement with the experimental results obtained by Waleed Mohamed Elsayed [45] (figure 12).

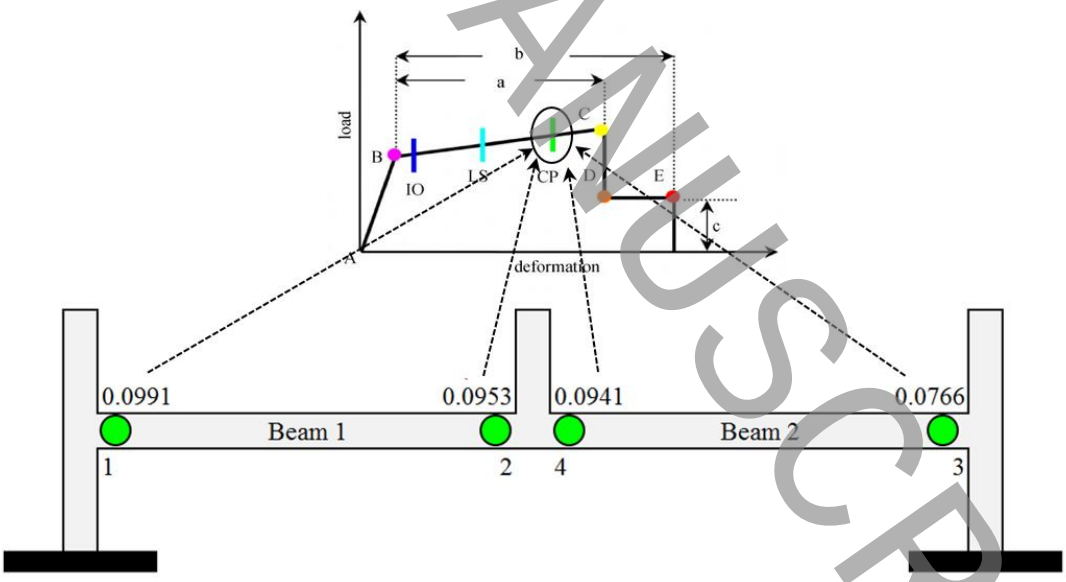

Fig. 11. Location of plastic hinges in the experimental RC Frame

a-Crack pattern of the RC frame

b-Failure of the top reinforcement of the beam

Fig. 12. Results obtained in the experimental test [45].

6. Study of the effect of removing a column in a frame.

The structure considered in this study is a three-story RC frame. The two upper stories height is 3.06 m whereas the ground floor height is 4.5 m as shown in figure 13. The considered frame structure is designed according to the specifications of the RPA seismic design code [50].

The mechanical characteristics of the materials (reinforcement and concrete) are summarized in table 7. The columns have a concrete cross-section of 30x30 cm² containing a 1.36% steel reinforcement ratio is 1.36% (Table 8). The beams for their part, have a cross-section of 30x35 cm² in all stories containing a steel reinforcement ratio of 0.87% (table 8).

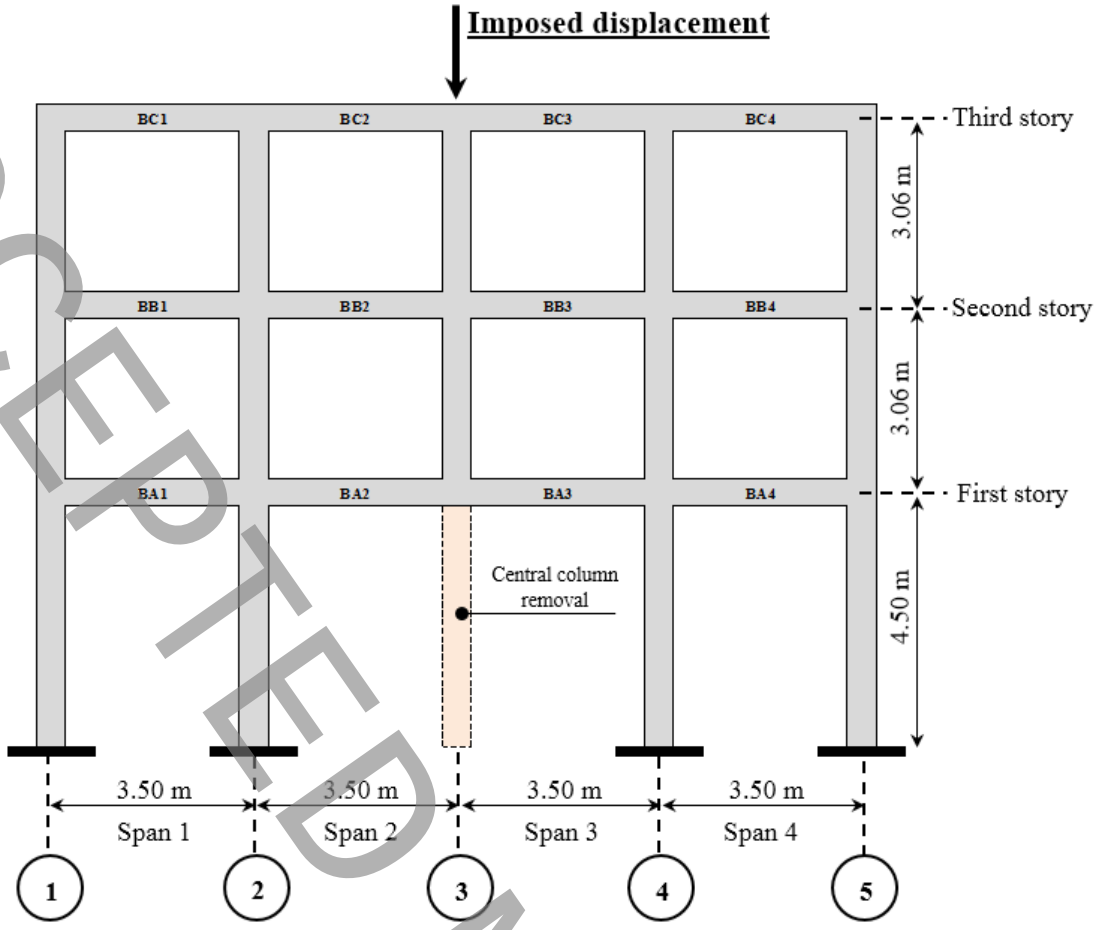

Fig. 13. Geometry and areas identification of the studied RCF structure subject to central-column removal.

Table 7. Mechanical properties of the materials.

Concrete		Steel	
Compressive stress (MPa)	Elasticity modulus (MPa)	Elasticity modulus (MPa)	Yield stress (MPa)
25	32164	200000	400

Table 8. Cross-section and reinforcement of the beams and columns

Columns	Beams
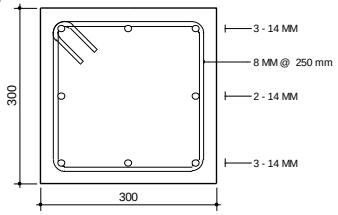	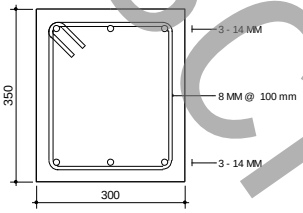
Reinforcement rebars	
8Φ14	6Φ14
Reinforcing ratio	
1.36 %	0.87 %

To view the positioning and the size of the plastic hinges in the beams of the RC frame structure. And to in order to reproduce the effect of the central column removal on the first floor, the RC frame has been subjected to an imposed displacement applied on its uppermost central column, that, with intensity gradually increasing (incrementally) [31, 40]. The increasing imposed displacement at which the various structural components reach failure is noted as a function of the roof vertical displacement. This incremental process continues until the ultimate structure displacement is obtained i.e., the occurrence of plastic hinges.

6-1- Failed column relationship (load-displacement)

Figure 14 shows the relationship between the applied load and the vertical displacement. As the vertical displacement increases, the load capacity rapidly increases. The applied load reached the maximum value of around 294 KN for a vertical displacement of 34 mm. Figure 14, shows that the overall response of the RC frame can be divided into four stages (see table 9).

Table 9. Stages of the global response of the RC frame structure

Fields	Segment	Definition
Elastic	OA	In this domain, the relationship between the load and the vertical displacement is linear, without any destruction affecting the RC frame.
Elastoplastic	AB	This is the beginning of the inelastic domain. The load is in a non-linear relationship with the displacement, and the structural stiffness begins to decrease at this stage. As the stress increases, the edges of the beams begin to crack, signaling the appearance of plastic hinges.
Plastic	BC	This domain is the stage of plastic hinge formation. Yielded sections at the edges of the beams have formed and the structure has progressively changed into a plastic stress system. The resistance to the progressive collapse of the frame began to decrease after reaching the maximum value of 294 KN.
Collapse	CD	In this domain, the bending capacity of the beams was practically lost and the edges of the beams are practically in an advanced state of yielding.

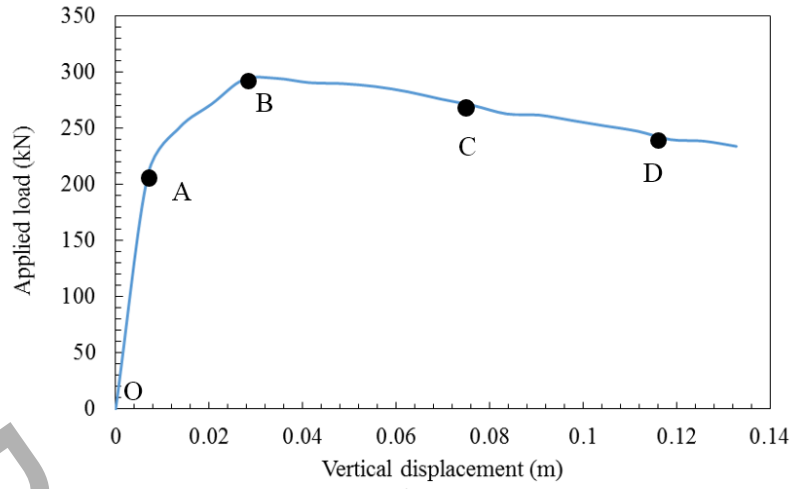

Fig. 14. Applied load versus vertical displacement of the beam-column joints at the uppermost central column

6-2- Results presentation

Table 10 shows the results in terms of plastic rotations developed in the beams adjacent to the center column after removing the latter from the first floor.

The resulting values of θ_p (plastic rotation) clearly show the presence of damaged areas at the edges of the beams, indicating the formation of plastic hinges in those beams.

The comparison between each domain provides information about the entry of plastic hinges in the plastic domain. The beams adjacent to the central column are the most damaged ones, with the maximum values of plastic rotation (0.0157 rad). The beams away from the central column area, exhibit better behavior in terms of plastic rotation (see table 10 and figure 15).

Table 10 shows the plastic rotation values. The beams of the first story have larger values of plastic rotations with a value of $\theta_p = 0.0157$ rad, due to the removal of the central column of the first story. Naturally, the beams of this story will suffer damages right after the beams of the uppermost story, with plastic rotation values ranging from 0.0154 to 0.0157 rad. In the beams of the other stories, there was minor damage, with plastic rotation values located in the range of 0.00882 to 0.06568 rad (Figure 15).

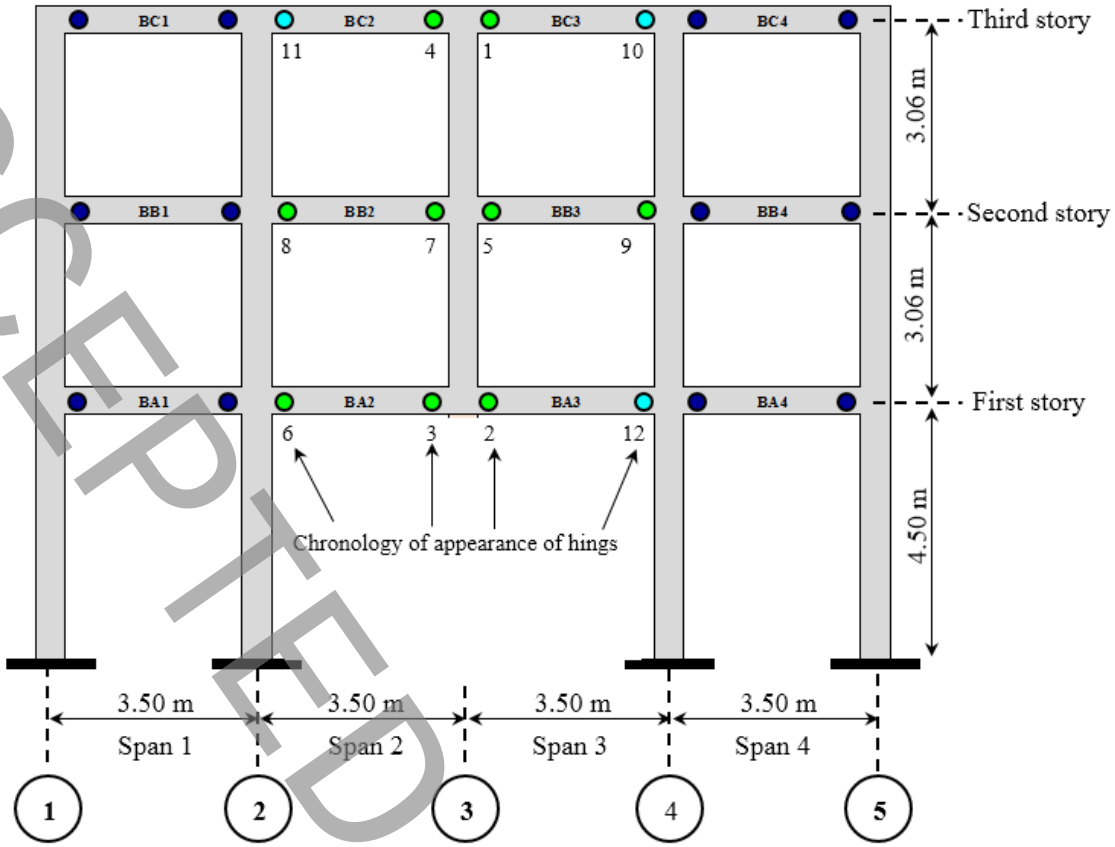

Fig. 15. Location of plastic hinges in the RCF structure and damage propagation

The final failure mode (appearance of plastic hinges) of the RC frame at the edges of the beams and their chronology of appearance is illustrated in figure 15. One can note that the plastic hinges are mainly concentrated in the edges of the beams adjacent to the central column (prevention of collapses), these zones sustain excessive internal stresses in particular a strong bending moment, which gives rise to an accumulation of plastic rotations fostering the appearance of plastic hinges, while the beams at the edges of the frame are slightly damaged (immediate occupancy).

Table 10. Values of plastic rotation in the beams of RCF

		Values of θp calculated with finite element model (rad)	θp according to FEMA 273 (rad)	Damage level by FEMA 273
First story	BA1	Elastic behavior is observed		Immediate Occupancy
	BA2	0.0128	θ(LS) < θp< θ(CP)	Collapse Prevention
	BA3	0.0154 0.0156 0.0081	θ(IO) < θp< θ(LS)	Life Safety
	BA4	Elastic behavior is observed θp < θ(IO)		Immediate Occupancy
Second story	BB1	Elastic behavior is observed θp < θ(IO)		Immediate Occupancy
	BB2	0.0117 0.0123	θ(LS) < θp< θ(CP)	Collapse Prevention
	BB3	0.0141 0.0104		
	BB4	Elastic behavior is observed θp < θ(IO)		Immediate Occupancy
Third story	BC1	Elastic behavior is observed θp < θ(IO)		Immediate Occupancy
	BC2	0.0084	θ(IO) < θp< θ(LS)	Life Safety
		0.0152	θ(LS) < θp< θ(CP)	Collapse prevention
	BC3	0.0157		
		0.0088	θ(IO) < θp< θ(LS)	Life Safety
	BC4	Elastic behavior is observed θp < θ(IO)		No damage

6-3- Evolution of vertical and horizontal displacements according to curvatures Cy

Figures 17, 18, and 19 show the evolution of vertical displacements as a function of the curvatures that develop in the zones adjacent to the central column (at the beams-columns joints, figure 16).

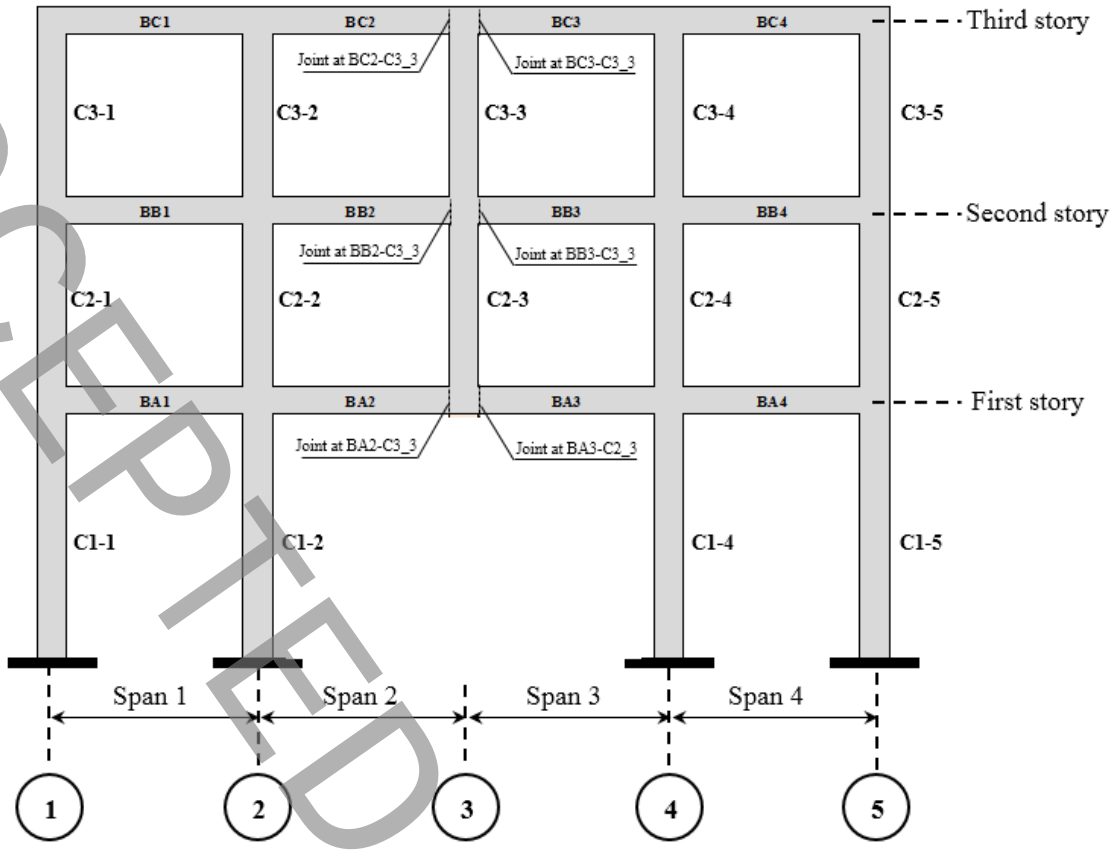

Fig. 16. Location of column-beam joints at the central column.

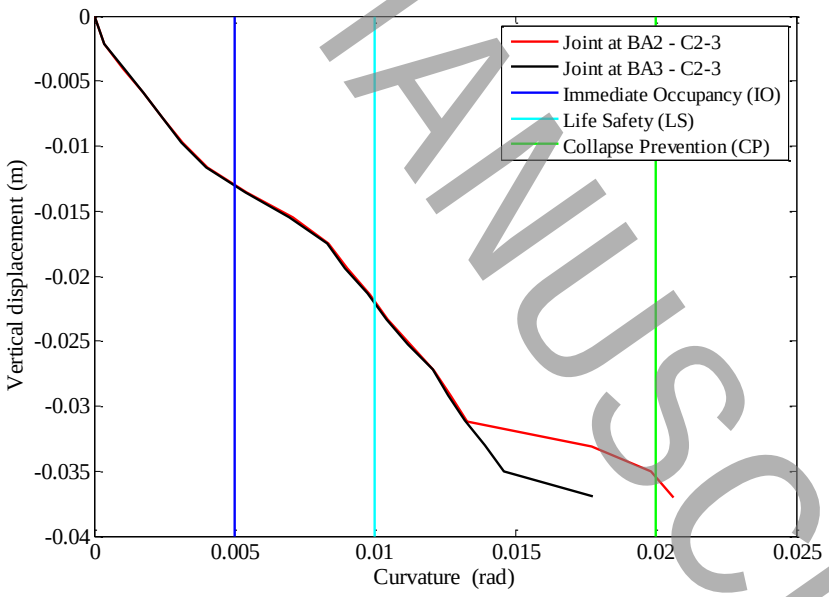

Fig. 17. Vertical displacement of joints versus curvature (first story).

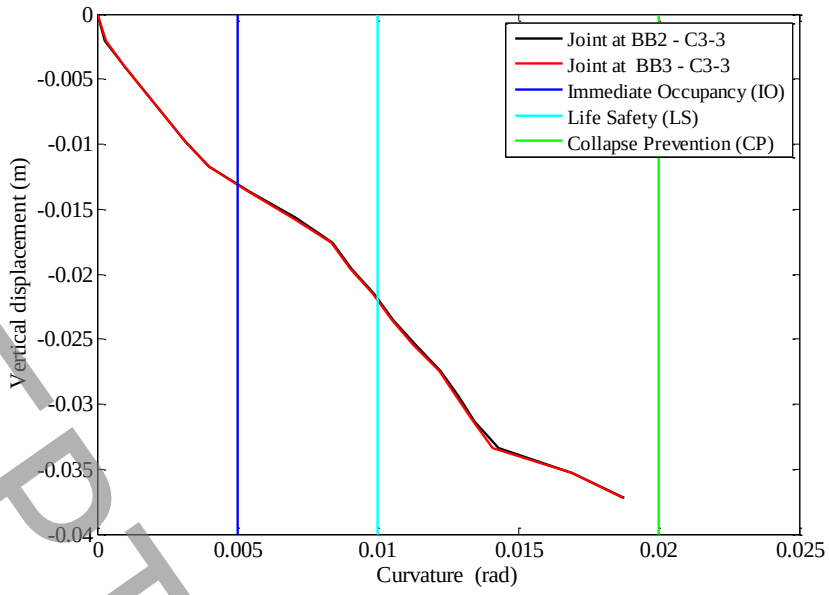

Fig. 18. Vertical displacement of joints versus curvature (second story).

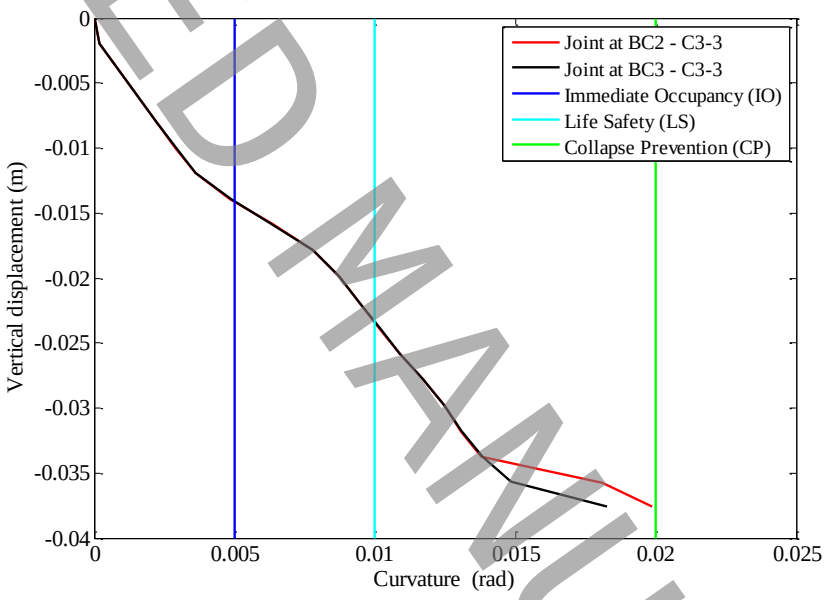

Fig. 19. Vertical displacement of joints versus curvature (third story).

Figures 17, 18, and 19 show the evolution of the curvatures as a function of the vertical displacements at the joints of the central column, calculated for the three considered stories. At the end of loading, the maximum vertical displacement obtained is of the order of 0.0372 m corresponding to a curvature range of 0.0177 to 0.0206 rad. This makes the edges of the central column adjacent beams the most vulnerable, as a consequence, gives rise to a high probability of occurrence of plastic hinges (LS to CP).

6-4- Horizontal and vertical displacements relationship of the beam-column joints

The relationship between horizontal and vertical joint displacements is shown in figures 20, 21, and 22. An increase in horizontal displacement indicates that the joint (beam-column connection) is moving away from the center column, while a decrease means that it is moving toward the center column.

With the emergence of plastic hinges in the beams, and as the vertical displacement increased, the adjacent beams of the central column tended to be more vulnerable, with a plastic rotation exceeding the life safety limit (LS), to enter the collapse prevention (CP) domain.

The horizontal displacements of the beam-column joints of the upper stories (2^{nd} and 3^{rd} story) similarly develop. Their displacements are slightly higher compared to the first story (Figures 20, 21, and 22). This explains why the frame enters the collapse phase, and the plastic hinges reach the collapse prevention CP domain.

Due to the progressive increase in horizontal displacements of the joints towards the inside or the outside of the central column, the forces (compression or tension) aggravate the formation of plastic hinges in the regions close to the edges of the beams, and the abrupt change in direction of the horizontal displacements fosters the damage to the joints, by cracking the concrete (Figures 20, 21 and 22).

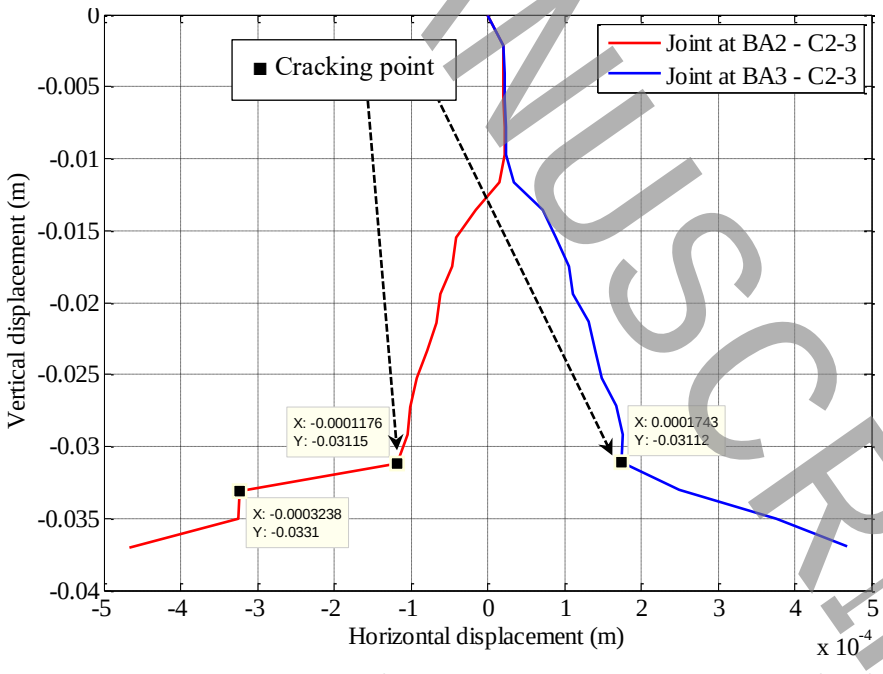

Fig. 20. Horizontal displacement of the joints between the beams and columns of the first story.

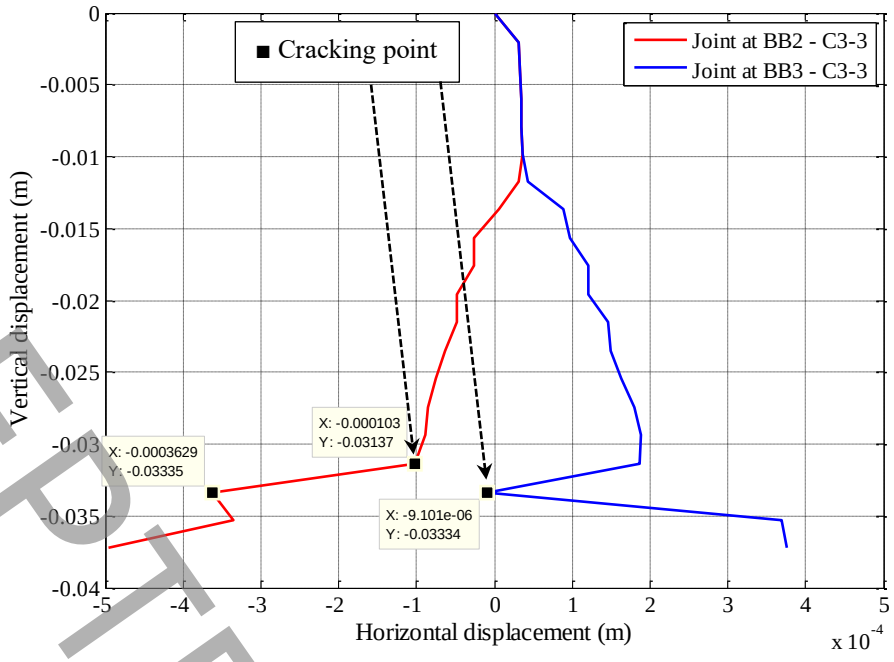

Fig. 21. Horizontal displacement of the joints between the beams and columns of the second story.

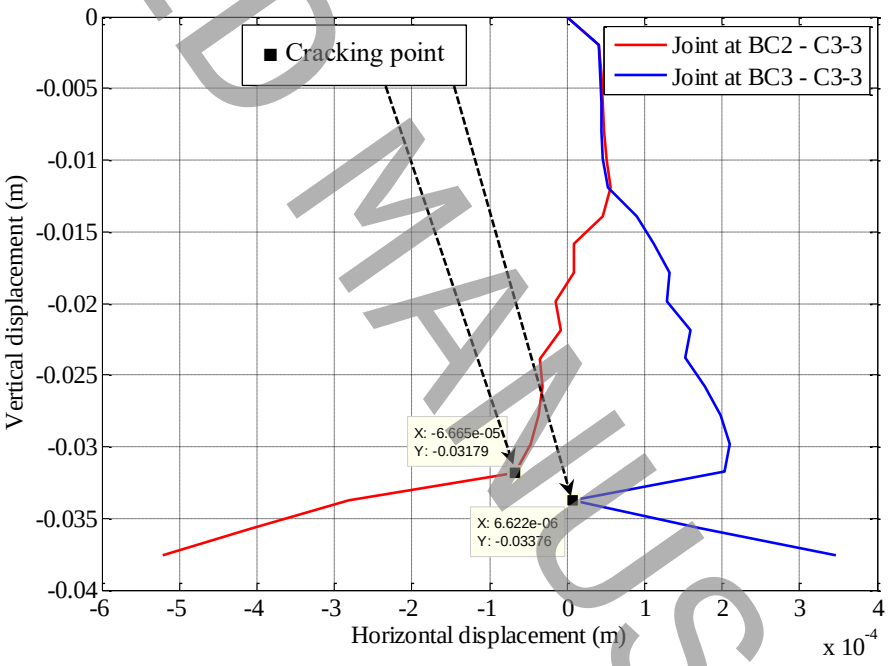

Fig. 22. Horizontal displacement of the joints between the beams and columns of the third story.

7. Conclusion

This paper presents a model for analyzing the collapse of reinforced concrete frames subjected to column failure (removal) scenarios. It is based on a damage assessment procedure that takes into account the combined effects of the bending forces in accordance with FEMA 273.

A CAST3M finite element code was used to investigate the response of a three-story, four-span reinforced concrete frame, based on the location and the quantification of damage through the evaluation of the size and type of the developed plastic hinges.

The final break-up mode (the appearance of plastic hinges) in the RC frame at the edges of the beams and the chronology of occurrence was illustrated. Those plastic hinges were mainly concentrated at the edges of the beams adjacent to the central column (personal safety or collapse prevention). These areas were subject to excessive internal stresses particularly in terms of bending moment, giving rise to an accumulation of plastic rotations, which foster the appearance of plastic hinges. The outer beams of the RC frame, oppositely, are slightly damaged (immediate occupancy). Since, the beams of the first story have higher values of plastic rotations, naturally, these beams will be damaged right after the beams of the last and the intermediate story.

The collapse of the structural component (the column) was correctly detected and predicted by the proposed modeling procedure. Therefore, the obtained results can provide new information regarding damage and failure assessment, in the analysis process of the RC frames progressive collapse. The modeling results also allow engineers to improve their design against a progressive collapse and to assess the plastic hinges locations that may appear under vertical load.

8. References

[1] A. Abbasi, P.J. Hogg, Fire testing of concrete beams with fibre reinforced plastic rebar, in: Advanced Polymer Composites for Structural Applications in Construction, Elsevier, 2004, pp. 445-456.
[2] C.W. Stover, J.L. Coffman, US Geological Survey Professional Paper 1527, United States Government Printing Office, Washington, (1993).
[3] M.S. Yarandi, M. Saatcioglu, S. Foo, Rectangular concrete columns retrofitted by external prestressing for seismic shear resistance, in: 13th World Conference on Earthquake Engineering. Vancouver, BC, Canada, 2004.
[4] K. Qian, S.-L. Liang, D.-C. Feng, F. Fu, G. Wu, Experimental and numerical investigation on progressive collapse resistance of post-tensioned precast concrete beam-column subassemblages, Journal of Structural Engineering, 146(9) (2020) 04020170.
[5] J. Yu, K.H. Tan, Structural behavior of reinforced concrete frames subjected to progressive collapse, ACI structural journal, 114(1) (2017) 63-74.
[6] J. Yu, Y.-P. Gan, J. Liu, Numerical study of dynamic responses of reinforced concrete infilled frames subjected to progressive collapse, Advances in Structural Engineering, 24(4) (2021) 635-652.
[7] X. Lu, K. Lin, D. Gu, Y. Li, Experimental Study of Novel Concrete Frames Considering Earthquake and Progressive Collapse, in: Concrete Structures in Earthquake, Springer, 2019, pp. 29-45.
[8] X. Lu, K. Lin, Y. Li, H. Guan, P. Ren, Y. Zhou, Experimental investigation of RC beam-slab substructures against progressive collapse subject to an edge-column-removal scenario, Engineering Structures, 149 (2017) 91-103.
[9] Z.P. Bažant, M. Verdure, Mechanics of progressive collapse: Learning from World Trade Center and building demolitions, Journal of Engineering Mechanics, 133(3) (2007) 308-319.

[10] M.M. Talaat, Computational modeling of progressive collapse in reinforced concrete frame structures, University of California, Berkeley, 2007.
[11] G. Kaewkulchai, E. Williamson, Modeling the impact of failed members for progressive collapse analysis of frame structures, Journal of Performance of Constructed Facilities, 20(4) (2006) 375-383.
[12] M. Sasani, A. Kazemi, S. Sagiroglu, S. Forest, Progressive collapse resistance of an actual 11-story structure subjected to severe initial damage, Journal of Structural Engineering, 137(9) (2011) 893-902.
[13] J. Yu, Y.-P. Gan, J. Wu, H. Wu, Effect of concrete masonry infill walls on progressive collapse performance of reinforced concrete infilled frames, Engineering structures, 191 (2019) 179-193.
[14] J. Yu, L. Luo, Y. Li, Numerical study of progressive collapse resistance of RC beam-slab substructures under perimeter column removal scenarios, Engineering Structures, 159 (2018) 14-27.
[15] W.-J. Yi, Q.-F. He, Y. Xiao, S.K. Kunnath, Experimental study on progressive collapse-resistant behavior of reinforced concrete frame structures, ACI Structural Journal, 105(4) (2008) 433.
[16] Q. Kai, B. Li, Q. He, W. Yi, Slab effects on response of reinforced concrete substructures after loss of corner column, ACI Struct. J, 109(6) (2012) 845-855.
[17] DoD, Design of buildings to resist progressive collapse, Unified Facilities Criteria (UFC) 4-023-03, (2009).
[18] U. Gsa, Progressive collapse analysis and design guidelines for new federal office buildings and major modernization projects, Washington, DC, (2003).
[19] K. Qian, S.-L. Liang, F. Fu, Q. Fang, Progressive collapse resistance of precast concrete beam-column sub-assemblages with high-performance dry connections, Engineering Structures, 198 (2019) 109552.
[20] E. Livingston, M. Sasani, M. Bazan, S. Sagiroglu, Progressive collapse resistance of RC beams, Engineering Structures, 95 (2015) 61-70.
[21] K. Khandelwal, S. El-Tawil, Assessment of progressive collapse residual capacity using pushdown analysis, in: Structures Congress 2008: Crossing Borders, 2008, pp. 1-8.
[22] T. Kim, J. Kim, J. Park, Investigation of progressive collapse-resisting capability of steel moment frames using push-down analysis, Journal of Performance of Constructed Facilities, 23(5) (2009) 327-335.
[23] Y. Li, X. Lu, H. Guan, L. Ye, An energy-based assessment on dynamic amplification factor for linear static analysis in progressive collapse design of ductile RC frame structures, Advances in Structural Engineering, 17(8) (2014) 1217-1225.
[24] K. Marchand, A. McKay, D.J. Stevens, Development and application of linear and non-linear static approaches in UFC 4-023-03, in: Structures Congress 2009: Don't Mess with Structural Engineers: Expanding Our Role, 2009, pp. 1-10.
[25] S. Kokot, A. Anthoine, P. Negro, G. Solomos, Static and dynamic analysis of a reinforced concrete flat slab frame building for progressive collapse, Engineering Structures, 40 (2012) 205-217.
[26] P. Ruth, K.A. Marchand, E.B. Williamson, Static equivalency in progressive collapse alternate path analysis: Reducing conservatism while retaining structural integrity, Journal of Performance of Constructed Facilities, 20(4) (2006) 349-364.
[27] T.C. Wang, Z.P. Li, Nonlinear static analysis for progressive collapse potential of RC building, in: Applied Mechanics and Materials, Trans Tech Publ, 2011, pp. 146-152.
[28] L. Kwasniewski, Nonlinear dynamic simulations of progressive collapse for a multistory building, Engineering Structures, 32(5) (2010) 1223-1235.
[29] E. Brunesi, R. Nascimbene, F. Parisi, N. Augenti, Progressive collapse fragility of reinforced concrete framed structures through incremental dynamic analysis, Engineering Structures, 104 (2015) 65-79.
[30] S. Marjanishvili, Progressive analysis procedure for progressive collapse, Journal of performance of constructed facilities, 18(2) (2004) 79-85.
[31] B.S.S. Council, NEHRP Commentary on the Guidelines for the Seismic Rehabilitation of Buildings (FEMA Publication 274), in, ATC-33 Project, Washington, DC, 1997.
[32] I. Bitar, S. Grange, P. Kotronis, N. Benkemoun, A review on various formulations of displacement based multi-fiber straight Timoshenko beam finite elements, in: CIGOS 2015-Conférence Internationale Géotechnique-Ouvrage-Structure, Innovations in Construction, 2015.
[33] D. Combescure, P. Pegon, Application of the local-to-global approach to the study of infilled frame structures under seismic loading, Nuclear engineering and design, 196(1) (2000) 17-40.
[34] A. Mortezaei, H.R. Ronagh, Plastic hinge length of FRP strengthened reinforced concrete columns subjected to both far-fault and near-fault ground motions, scientia iranica, 19(6) (2012) 1365-1378.
[35] A.L.L. Baker, The ultimate-load theory applied to the design of reinforced & prestressed concrete frames, Concrete Publications, 1956.
[36] O. Bayrak, S.A. Sheikh, Confinement reinforcement design considerations for ductile HSC columns, Journal of Structural Engineering, 124(9) (1998) 999-1010.
[37] A. Baker, A. Amarakone, N. Inelastic hyperstatic frame analysis, ACI Structural Journal, (1964) 85-142.
[38] M.P. Berry, D.E. Lehman, L.N. Lowes, Lumped-plasticity models for performance simulation of bridge columns, ACI Structural Journal, 105(3) (2008) 270.

[39] W.G. Corley, Rotational capacity of reinforced concrete beams, Journal of the Structural Division, 92(5) (1966) 121-146.
[40] C.D. Comartin, R.W. Niewiarowski, S.A. Freeman, F.M. Turner, Seismic evaluation and retrofit of concrete buildings: a practical overview of the ATC 40 Document, Earthquake Spectra, 16(1) (2000) 241-261.
[41] M.H. Scott, G.L. Fenves, Plastic hinge integration methods for force-based beam–column elements, Journal of Structural Engineering, 132(2) (2006) 244-252.
[42] A.A. KHEYR, A. Mortezaei, The effect of element size and plastic hinge characteristics on nonlinear analysis of RC frames, (2008).
[43] S. Bae, O. Bayrak, Plastic hinge length of reinforced concrete columns, ACI Structural Journal, 105(3) (2008) 290.
[44] A. Kahil, A. Nekmouche, S. Boukais, M. Hamizi, N.E. Hannachi, Effect of RC wall on the development of plastic rotation in the beams of RC frame structures, Frontiers of Structural and Civil Engineering, 12(3) (2018) 318-330.
[45] W.M. Elsayed, M.A. Abdel Moaty, M.E. Issa, Effect of reinforcing steel debonding on RC frame performance in resisting progressive collapse, HBRC journal, 12(3) (2016) 242-254.
[46] E. Hognestad, Study of combined bending and axial load in reinforced concrete members, University of Illinois at Urbana Champaign, College of Engineering …, 1951.
[47] J.K. Wight, J.G. Macgregor, Reinforced Concrete Mechanics and Design, 2012, in, Pearson Education, Inc., Upper Saddle River, New Jersey.
[48] P. Kotronis, L. Davenne, J. Mazars, Poutre multifibre Timoshenko pour la modélisation de structures en béton armé: Théorie et applications numériques, Revue française de génie civil, 8(2-3) (2004) 329-343.
[49] J.P.S.C.d.M. Guedes, Seismic behaviour of reinforced concrete bridges: Modelling, numerical analysis and experimental assessment, (1997).
[50] R. Taleb, Règles Parasismiques Algériennes RPA 99-Version 2003 pour les Structures de Bâtiments en Béton Armé: Interprétations et Propositions.